

Selective Rydberg pumping via strong dipole blockade

Xiao-Qiang Shao^{1,2,*}

¹Center for Quantum Sciences and School of Physics, Northeast Normal University, Changchun 130024, China

²Center for Advanced Optoelectronic Functional Materials Research,
and Key Laboratory for UV Light-Emitting Materials and Technology of Ministry of Education,
Northeast Normal University, Changchun 130024, China

The resonant dipole-dipole interaction between highly excited Rydberg levels dominates the interaction of neutral atoms at short distances scaling as $1/r^3$. Here we take advantage of the combined effects of strong dipole-dipole interaction and multifrequency driving fields to propose one type of selective Rydberg pumping mechanism. In the ground state space of two atoms $\{|00\rangle, |01\rangle, |10\rangle, |11\rangle\}$, this mechanism allows $|11\rangle$ to be resonantly pumped upwards to the single-excited Rydberg states while the transitions of the other three states are suppressed. From the perspective of mathematical form, we achieve an analogous Föster resonance for ground states of neutral atoms. Thence we apply this mechanism to one-step implementation of controlled- Z gate, realization of ground-state blockade, and speedup preparation of maximally entangled state with dissipation, and further discuss respectively each feasibility with the state-of-the-art technology.

I. INTRODUCTION

Rydberg blockade and Rydberg antiblockade are two representative phenomena observed in neutral atom systems [1–6]. The former prevents two or more atoms from being resonantly excited to the Rydberg state due to the strong Rydberg-Rydberg interaction (RRI), while the later permits a resonant two-photon transition as the shifting energy of Rydberg states is compensated by the two-photon detuning. In addition to the above two characteristics, the highly excited Rydberg states possess a long lifetime proportional to the third power of the principle quantum number [7–9], which makes them very suitable for encoding qubits or as a medium in the field of quantum information science [10–21].

Nevertheless, the spontaneous emission of Rydberg state cannot be ignored once the long-time dynamic evolution is considered, such as a process of a many-body system reaching equilibrium. Using a continuous laser field coupling the ground state to the Rydberg state can form two dressed states, these Rydberg-dressed states have relative long lifetimes as compared to the bare Rydberg state, while maintains a certain strength of the RRI to induce the blockade effect [22, 23]. Therefore the Rydberg dressing technique provides a tunable interaction for quantum control and quantum computing [24–33]. It should be emphasized that at the end of each Rydberg-dressed scheme, an additional operation that adiabatically transferring the Rydberg-dressed state back to the ground state is necessary to avoid further decoherence.

Different from the Rydberg dressing techniques, the spontaneous emission of the Rydberg state can be neglectable during the whole process of the ground-state blockade mechanism [34]. The transitions between ground states governed by the weak Raman couplings are “frequently measured” by a strong Rydberg antiblockade interaction. Thence the Rydberg states are virtually excited and the population of a two-atom ground state that directly coupled to the two-atom Rydberg state is blocked. The prominent advantage of the ground-

state blockade is that although the strength of the Rydberg antiblockade is usually much smaller than the Rabi coupling of Rydberg atoms, it can be made far greater than the Raman coupling of ground state, and simultaneously reduces the atomic spontaneous emission for the Raman coupling dynamics [35, 36].

In this paper, we aim to engineer an alternative interaction mechanism for neutral atom systems, which is able to replace the traditional second-order dynamics in the Rydberg antiblockade with first-order interaction strength. This idea mainly comes from our precious work about the unconventional Rydberg pumping (URP) [37], where the evolution of two atoms initialized in the same ground state is frozen even under driven by laser fields. Instead of using the van der Waals interaction of Rydberg atoms for URP, here we take advantage of the combined effects of strong dipole-dipole interaction (which is not replaceable) and multifrequency driving fields to propose a selective Rydberg pumping (SRP) mechanism, i.e., in the ground state space of two atoms $\{|00\rangle, |01\rangle, |10\rangle, |11\rangle\}$, this mechanism allows $|11\rangle$ to be resonantly pumped upwards to the single-excited Rydberg states while the transitions of the other three states are suppressed. Since the dynamics is dominated by the first-order Rabi coupling of Rydberg atoms, our work may have a great application value on speeding up the Rydberg-antiblockade-based schemes [12, 13, 20, 34].

The structure of the paper is organized as follows. In Sec. II, we first illustrate the mechanism of the SRP in detail and explain why the dipole-dipole interaction of Rydberg atoms cannot be replaced by the van der Waals interaction. In Sec. III, we then apply the technology of SRP to one-step implementation of controlled- Z gate, realization of ground-state blockade, and dissipative preparation of maximally entangled state with available experimental parameters and compare them with the relevant Rydberg-antiblockade-based schemes. In Sec. IV, we further discuss the effects of imperfection such as Föster defect and decoherence on the performance of the SRP, and finally give a summary of our manuscript in Sec. V.

* shaoxq644@nenu.edu.cn

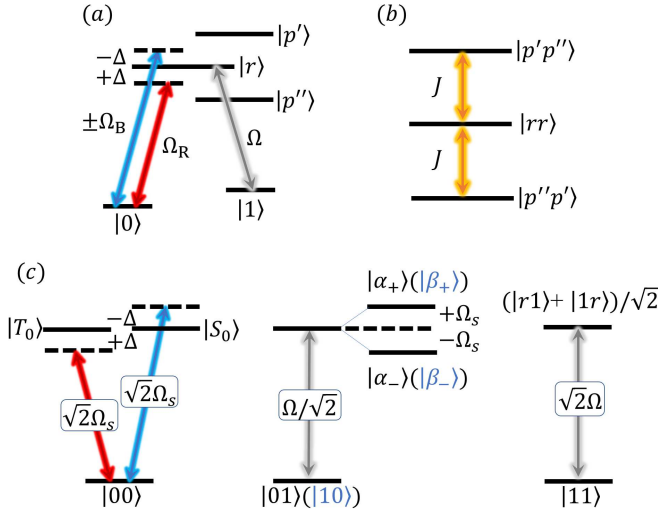


FIG. 1. Schematic view of the atomic-level configuration. (a) Each atom is driven by three types of laser fields. The ground state $|0\rangle$ is dispersively coupled to the Rydberg state $|r\rangle$ by one laser field with Rabi frequency $\pm\Omega_B$ (which is blue-detuned by Δ) and another laser field with Rabi frequency Ω_R (which is red-detuned by Δ), simultaneously. While the transition between $|1\rangle$ and $|r\rangle$ is driven by a resonant laser field with Rabi frequency Ω . (b) The dipole-dipole (Föster resonance) interaction of the highly excited Rydberg states. (c) The effective transitions for the ground states, where $|T_0\rangle(|S_0\rangle) = (|r0\rangle \pm |0r\rangle)/\sqrt{2}$. In the regime of large detuning ($\Delta = \sqrt{2}J \gg \Omega_s \gg \Omega$), there is only one resonantly coherent oscillation between state $|11\rangle$ and the single-excited Rydberg states.

II. MECHANISM

The system considered here incorporates two multilevel atoms with the same configuration as adopted in Ref. [2]. Each atom consists of two ground states $|0\rangle$ and $|1\rangle$, and three long-lived Rydberg states $|r\rangle$, $|p'\rangle$, and $|p''\rangle$ as shown in Fig. 1(a). The ground state $|0\rangle$ is dispersively coupled to the Rydberg state $|r\rangle$ by one laser field with Rabi frequency $\pm\Omega_B$ (“+” for atom 1 and “-” for atom 2), blue-detuned by Δ , and another laser field with Rabi frequency Ω_R , red-detuned by Δ , simultaneously. While the transition between $|1\rangle$ and $|r\rangle$ is driven by a resonant laser field with Rabi frequency Ω . The resonant dipole-dipole interactions between Rydberg atoms (Föster resonance interaction) is illustrated in Fig. 1(b), which characterizes a hopping transition between a pair of Rydberg states with strength J . In the interaction picture, the Hamiltonian of the system reads ($\hbar = 1$)

$$H_I = \sum_{n=1}^2 \Omega |1\rangle_n \langle r| + \left\{ \Omega_R e^{-i\Delta t} + \Omega_B e^{i[\Delta t + (n-1)\pi]} \right\} |0\rangle_n \langle r| + J |rr\rangle (\langle p'p''| + \langle p''p'|) + \text{H.c.} \quad (1)$$

In general the strong dipole-dipole interaction between Rydberg atoms can result in a splitting of the excited Rydberg components, thus this part can be reformulated in the diagonal form $\sqrt{2}J(|E_+\rangle\langle E_+| - |E_-\rangle\langle E_-|)$, where $|E_\pm\rangle = [\sqrt{2}|rr\rangle \pm (|p'p''\rangle + |p''p'\rangle)]/2$ are the eigenstates of the Ryd-

berg interaction. For the sake of convenience, we suppose all the Rabi frequencies are real and set $\Omega_B = \Omega_R = \Omega_s$, then using the collective states of two atoms with respect to a rotating frame $U = \exp[-\sqrt{2}iJt(|E_+\rangle\langle E_+| - |E_-\rangle\langle E_-|)]$, the above Hamiltonian is written as

$$\begin{aligned} H_I &= H_1 + H_2, \quad (2) \\ H_1 &= \sqrt{2}\Omega_s [|00\rangle (\langle T_0| e^{-i\Delta t} + \langle S_0| e^{i\Delta t}) \\ &\quad + |01\rangle \left[\frac{\Omega}{\sqrt{2}} (\langle T_0| - \langle S_0|) + 2\Omega_s \cos(\Delta t) \langle r1| \right] \\ &\quad + |10\rangle \left[\frac{\Omega}{\sqrt{2}} (\langle T_0| + \langle S_0|) - 2i\Omega_s \sin(\Delta t) \langle 1r| \right] \\ &\quad + \Omega |11\rangle (\langle r1| + \langle 1r|) + \text{H.c.}, \\ H_2 &= \Omega_s |T_0\rangle [\langle E_+| e^{-i(\Delta + \sqrt{2}J)t} + \langle E_-| e^{-i(\Delta - \sqrt{2}J)t}] \\ &\quad - \Omega_s |S_0\rangle [\langle E_+| e^{i(\Delta - \sqrt{2}J)t} + \langle E_-| e^{i(\Delta + \sqrt{2}J)t}] \\ &\quad + \frac{\Omega}{\sqrt{2}} (|r1\rangle + |1r\rangle) (\langle E_+| e^{-\sqrt{2}iJt} + \langle E_-| e^{\sqrt{2}iJt}) \\ &\quad + \text{H.c.}, \end{aligned}$$

where H_1 describes the interaction between ground states and single-excited Rydberg states, and H_2 bridges the transitions of single-excited and two-excited Rydberg states. In the regime of the large detuning limits $\Delta = \sqrt{2}J$ and $\Delta \gg \{\Omega_s, \Omega\}$, the terms oscillating with high frequencies $\{\pm\Delta, \pm\sqrt{2}J, \pm(\Delta + \sqrt{2}J)\}$ in Eq. (2) can be safely disregarded, then we have a concise form as

$$\begin{aligned} H_I &= \Omega |11\rangle (\langle r1| + \langle 1r|) + \frac{\Omega}{\sqrt{2}} |01\rangle (\langle T_0| - \langle S_0|) \\ &\quad + \frac{\Omega}{\sqrt{2}} |10\rangle (\langle T_0| + \langle S_0|) + \Omega_s |T_0\rangle \langle E_-| \\ &\quad - \Omega_s |S_0\rangle \langle E_+| + \text{H.c.} \quad (3) \end{aligned}$$

This Hamiltonian can be further simplified by considering the limitation of $\Omega_s \gg \Omega$. Analogous to the process of dipole blockade, the strong Rabi coupling Ω_s leads to large shifting energies of states $|T_0\rangle$ and $|S_0\rangle$, which is big enough to block the jumps from $|01\rangle$ ($|10\rangle$) towards to the excited states driven by Rabi frequency Ω . Most importantly, there is no extra stark shifts or detuning-induced Raman resonance, because these transition paths mediated by the independent channels $|\alpha_\pm\rangle$ and $|\beta_\pm\rangle$ interfere destructively, where

$$\begin{aligned} |\alpha_\pm\rangle &= \frac{1}{2} [(|T_0\rangle - |S_0\rangle) \pm (|E_+\rangle + |E_-\rangle)], \\ |\beta_\pm\rangle &= \frac{1}{2} [(|T_0\rangle + |S_0\rangle) \mp (|E_+\rangle - |E_-\rangle)], \end{aligned}$$

are the corresponding eigenstates of the part governed by Ω_s . Therefore the Hamiltonian of our current model reduces to an effective form

$$H_{\text{eff}} = \Omega |11\rangle (\langle r1| + \langle 1r|) + \text{H.c.} \quad (4)$$

Now we finish the mechanism of SRP. The effective transitions for all ground states are also displayed in Fig. 1(c) in order to offer a better physical picture. Note that there are many

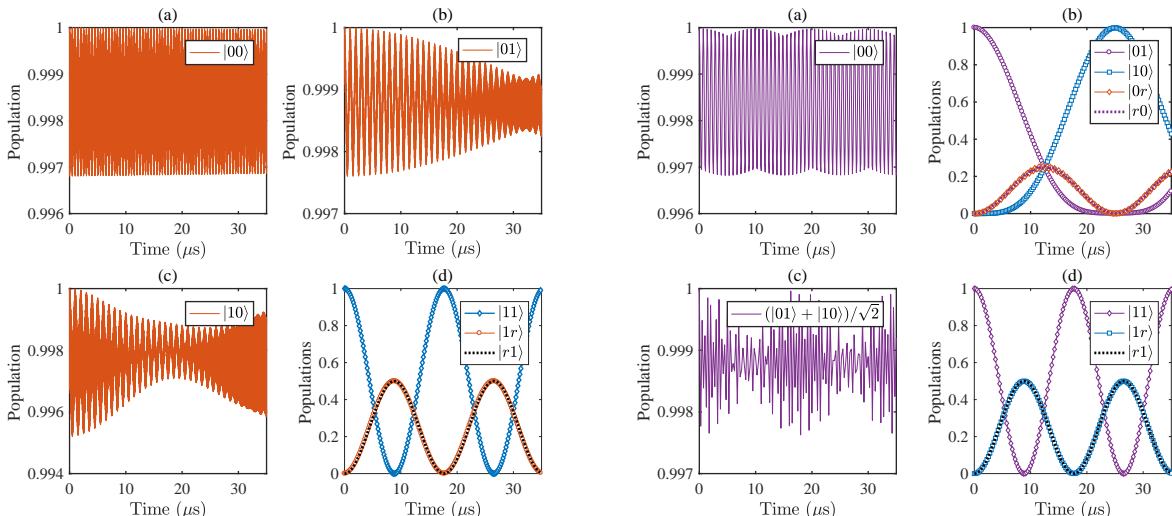


FIG. 2. Left panel: The temporal evolution of populations for different ground states governed by the full Hamiltonian Eq. (1). The parameters are chosen as $\Omega/2\pi = 0.02$ MHz, $\Omega_s/2\pi = 1$ MHz, and $J/2\pi = 50$ MHz. Right panel: The corresponding numerical simulations under the van der Waals interaction.

interesting features implied in Eq. (4). From the perspective of mathematical form, it describes an analogous Föster resonance, where the ground states $|11\rangle$ are coupled to other two states resonantly. So one potential application of our SRP is to simulate the Föster resonance-related phenomena with ground states of neutral atoms. In addition, the first-order Rabi coupling is usually much larger than the second-order interaction as required by the Rydberg antiblockade, the SRP mechanism may greatly speed up the Rydberg-antiblockade-based schemes, while reducing the decay of other excited Rydberg states.

Before we go on to the next step, let us first discuss the feasibility of the SRP with typical parameters used in experiments. According to the works of Browaeys *et al.* [38, 39], the Föster resonance of excited Rydberg states is reached using $|p'\rangle = |61P_{1/2}, m_J = 1/2\rangle$, $|r\rangle = |59D_{3/2}, m_J = 3/2\rangle$, and $|p''\rangle = |57F_{5/2}, m_J = 5/2\rangle$ of two ^{87}Rb atoms in the presence of an electric field and the measured $C_3/2\pi = 2.39 \pm 0.03$ GHz μm^3 which is close to the theoretical value $C_3/2\pi \simeq 2.54$ GHz μm^3 . This allows the dipole interaction strength $J/2\pi$ to be continuously varied between 2.39 MHz and 152.96 MHz corresponding to the distance between atoms are adjusted from 10 μm to 2.5 μm . The Rabi coupling of the ground states and the Rydberg states is accomplished by a tunable two-photon process that can be up to $2\pi \times 5$ MHz in Ref. [39]. So the condition for realization of the SRP ($\Delta = \sqrt{2}J \gg \Omega_s \gg \Omega$) is easy to access by choosing $\Omega/2\pi = 0.02$ MHz, $\Omega_s/2\pi = 1$ MHz, and $J/2\pi = 50$ MHz. In the left panel of Fig. 2, we depict the temporal evolution of all ground states obtained from the full Hamiltonian of Eq. (1). It can be seen that this result has an excellent agreement with our prediction. The states $|00\rangle$, $|01\rangle$, and $|10\rangle$ always keep in their initial states with fidelities higher than 99.5% during the coherent-oscillation process of states $|11\rangle$

and $(|r1\rangle + |1r\rangle)/\sqrt{2}$. As we mentioned earlier, the dipole-dipole interaction is the key factor to implement the SRP, which cannot be substituted by the van der Waals-type interaction. In the right panel of Fig. 2 we also analyze the dynamical behavior of each ground state based on the van der Waals interaction ($U = J = 2\pi \times 50$ MHz) as a comparison. In this case, the energy of the excited Rydberg states will only shift without splitting, which results in an undesired resonant transition between states $(|01\rangle - |10\rangle)/\sqrt{2}$ and $(|0r\rangle - |r0\rangle)/\sqrt{2}$.

III. APPLICATIONS

A. Controlled- Z gate

The mechanism of SRP itself defines a kind of quantum logic operation, *i.e.* $|00\rangle \rightarrow |00\rangle$, $|01\rangle \rightarrow |01\rangle$, $|10\rangle \rightarrow |10\rangle$, and $|11\rangle \rightarrow \cos(\sqrt{2}\Omega t)|11\rangle + i \sin(\sqrt{2}\Omega t)(|r1\rangle + |1r\rangle)/\sqrt{2}$. Thus the two-qubit controlled- Z gate corresponding $\sqrt{2}\Omega t = \pi$ is readily implemented only in one step. Without loss of generality, we use the fidelity between quantum states $\langle \psi_{\text{ideal}} | \rho(t) | \psi_{\text{ideal}} \rangle$ as a measure to check the performance of the gate, where the initial (ideal final state) is $(|00\rangle + |01\rangle + |10\rangle \pm |11\rangle)/2$. In Fig. 3(a) we employ the same group of parameters used in Fig. 2 to obtain a nearly perfect two-qubit controlled- Z gate with fidelity of 99.9% at $t = 17.7$ μs . In Fig. 3(b) we further enhance the Rabi frequency of the resonant driving field to $\Omega/2\pi = 0.06$ MHz, which thence shortens the gating time at the expense of just decreasing the performance of the quantum gate by 0.11%. And the parameters used in Fig. 3(c) guarantees a more faster implementation of logic gate at $t = 2.36$ μs with a fidelity of 99.31%. Compared with the schemes of Ref. [34, 40], our work does provide a way to perform quantum information processing quickly with

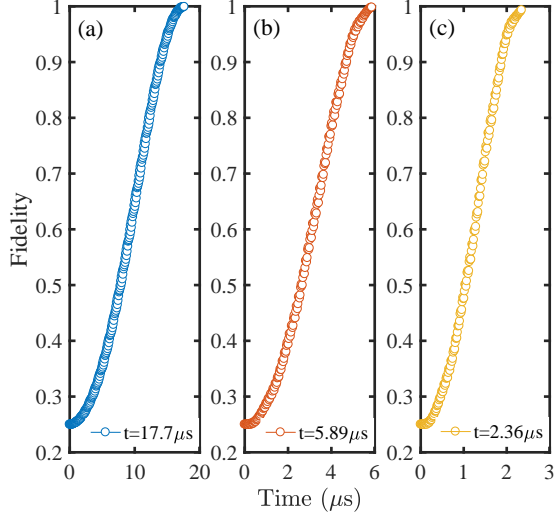


FIG. 3. The fidelity of the controlled-Z gate with quantum information encoded onto the ground states of neutral atoms. (a) The parameters are chosen as $\Omega/2\pi = 0.02$ MHz, $\Omega_s/2\pi = 1$ MHz, and $J/2\pi = 50$ MHz. (b) The parameters are chosen as $\Omega/2\pi = 0.06$ MHz, $\Omega_s/2\pi = 1$ MHz, and $J/2\pi = 50$ MHz. (c) The parameters are chosen as $\Omega/2\pi = 0.15$ MHz, $\Omega_s/2\pi = 2$ MHz, and $J/2\pi = 100$ MHz.

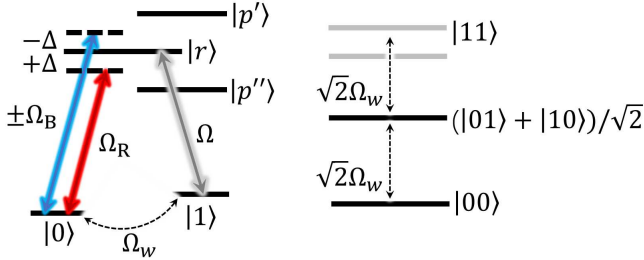


FIG. 4. Schematic view of the interactions between atoms and external driving fields for ground-state blockade.

available experimental parameters.

B. Ground-state blockade

Due to the resemblance between the Föster resonance interaction and our SRP, it is natural to extend the effect of Rydberg blockade to the ground states. Now we introduce a weak interaction Ω_w driving the transition between ground states, which can be realized directly by a Raman laser field or microwave field [28]. In this case the effective Hamiltonian of system is

$$H_{\text{eff}} = \sum_{n=1}^2 \Omega_w |0\rangle_n \langle 1| + \Omega |11\rangle (\langle r1| + \langle 1r|) + \text{H.c.}, \quad (5)$$

where the energy of state $|11\rangle$ in the ground state space is splitted by coupling to the single-excited Rydberg state, as shown in Fig. 4. If the Rabi coupling strength Ω is much

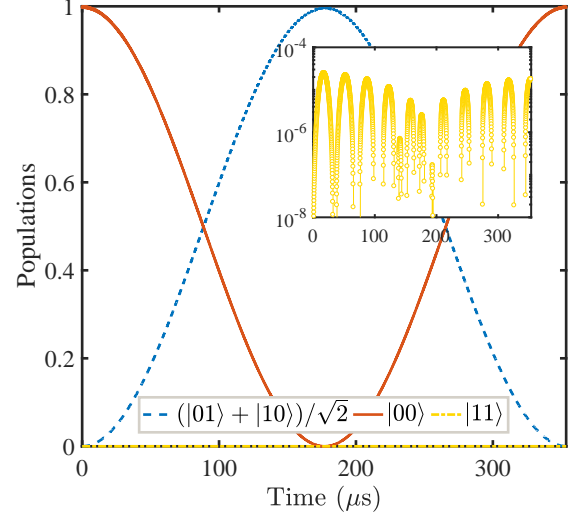


FIG. 5. The ground-state blockade induced by the selective Rydberg pumping. The inset shows the enlarged view of the population for state $|11\rangle$. The Rabi frequency of the laser field that acts on the ground state space is chosen as $\Omega_w/2\pi = 0.001$ MHz, and the other parameters are the same as in Fig. 2.

larger than the weak driving strength Ω_w , the population of state $|11\rangle$ will be blocked, and the evolution of atoms is confined to the subspace $\{|00\rangle, |01\rangle, |10\rangle\}$ governed by $H_{gb} = \Omega_w |00\rangle (\langle 01| + \langle 10|) + \text{H.c.}$. Fig. 5 characterizes the evolutions of all ground states beginning with state $|00\rangle$. The weak Raman coupling is selected as $\Omega_w/2\pi = 0.001$ MHz, and other parameters are the same as in Fig. 2. It clearly shows the phenomenon of ground-state blockade because the population of state $|11\rangle$ is suppressed well below the order of 10^{-4} during the whole process.

C. Steady entanglement

A maximally entangled state of two Rydberg atoms in the form of $(|01\rangle + |10\rangle)/\sqrt{2}$ can be produced through the ground-state blockade effect, as illustrated by the dashed line of Fig. 5. This unitary-dynamics-based protocol requires to exactly tailor the initial state and precisely control the interaction time. In contrast, the reservoir-engineering approaches to entanglement generation is able to release the above two restrictions by converting the decoherence factor into a resource [12–14, 19, 41–44]. On the basis of the previous model of Fig. 4, we consider the dissipative dynamics of system described by the effective master equation

$$\dot{\rho} = -i[H_{\text{eff}}, \rho] + \sum_{n=1}^2 \sum_{k=0}^1 L_n^k \rho L_n^{k\dagger} - \frac{1}{2} (L_n^{k\dagger} L_n^k \rho + \rho L_n^{k\dagger} L_n^k) \quad (6)$$

where H_{eff} is the Hamiltonian of Eq. (5) and $L_n^{0(1)} = \sqrt{\Gamma/2} |0(1)\rangle_n \langle r|$ is the Lindblad operator indicating the atom decay from the excited Rydberg state $|r\rangle$ into ground states $|0\rangle$

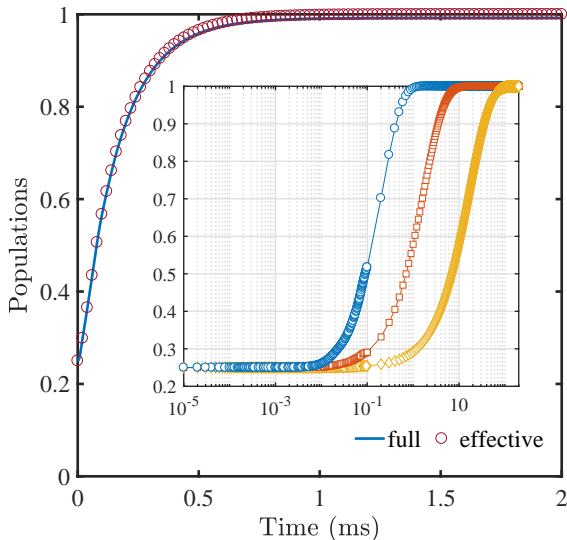


FIG. 6. The time evolution of population for the target state governed by the full and effective master equations. The initial state is a fully mixed state $\rho_0 = \sum_{i,j=0,1} |ij\rangle\langle ij|/4$, and the relevant parameters are set as $\Omega_w/2\pi = 0.005$ MHz, $\Omega/2\pi = 0.01$ MHz, $\Omega_s/2\pi = 1$ MHz, $\gamma/2\pi = 0.03$ MHz, and $J = 100$ MHz. The inset reflects the effect of different values of γ on the convergence time of entanglement, where the blue circle denotes $\gamma = 0.1$ MHz, the red square represents $\gamma = 0.01$ MHz, and the yellow rhombic corresponds to $\gamma = 0.001$ MHz.

and $|1\rangle$ with the same branching ratio $\gamma/2$. A simple inspection shows that the singlet state $(|01\rangle - |10\rangle)/\sqrt{2}$ is the unique stationary state solution of Eq. (6). In the inset of Fig. 6, we investigate the influence of different spontaneous emission rates on the convergence time of the maximally entangled state by fixing other parameters as $\Omega_w/2\pi = 0.005$ MHz, $\Omega/2\pi = 0.01$ MHz from an fully mixed state $\rho_0 = \sum_{i,j=0,1} |ij\rangle\langle ij|/4$. It reveals that a large decay rate can accelerate the convergence time. For example, the choice of $\gamma = 0.1$ MHz ensures a fidelity of 99.39% is achievable at $t = 1$ ms (blue circle), while a selection of $\gamma = 0.001$ MHz delay the time to 100 ms (yellow rhombic). We know the effective lifetime of Rb $59D_{3/2}$ Rydberg states is about 0.2 ms ($\gamma = 5$ kHz) at $T = 0$ K [45], whose convergence time can be inferred to be 20 ms according to the above discussion. Fortunately the lifetime of Rydberg state is adjustable utilizing the method of engineered spontaneous emission [19, 46]. By coupling the Rydberg state to a short-lived state (decay rate Γ) with a weak driving field Ω_d , we may obtain an extra effective decay rate for the Rydberg state as $4\Omega_d^2/\Gamma$. Therefore we find a fast way to dissipatively produce the maximally entangled state of two atoms using $\gamma/2\pi = 0.03$ MHz in Fig. 6, and the dynamics described by the full master equation is consistent with the effective prediction.

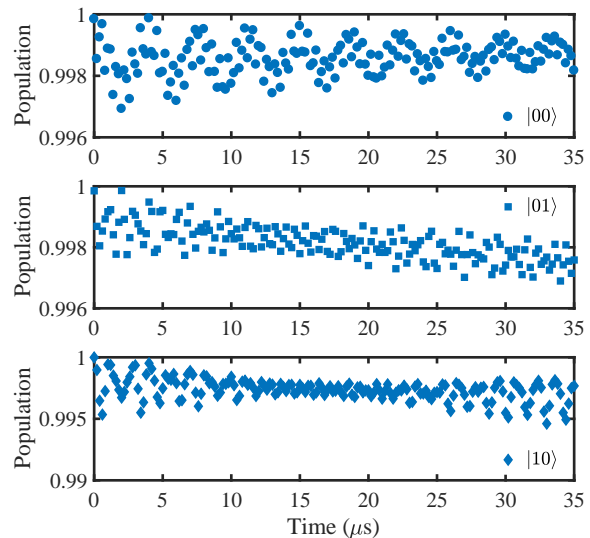


FIG. 7. The temporal evolution of populations for states $|00\rangle$, $|01\rangle$, and $|10\rangle$ in the presence of Föster defect $\delta/2\pi = 8.5$ MHz, and the other parameters are the same as in Fig. 2.

IV. INFLUENCE OF IMPERFECTION

In the presence of Föster defect, the dipole-dipole coupling between two Rydberg states $|rr\rangle$ and $(|p'p''\rangle + |p''p'\rangle)/\sqrt{2}$ in Eq. (1) is modified by

$$H_{dd} = \begin{pmatrix} 0 & \sqrt{2}J \\ \sqrt{2}J & \delta \end{pmatrix}, \quad (7)$$

where the δ is the Föster defect measuring the detuning of the above two states, and its value is only $2\pi \times 8.5$ MHz in the absence of an electric field [38]. This Föster defect alters the eigenvalues of the dipole-dipole interaction and then bring about a deviation $\epsilon = |\Delta = \sqrt{2}J - (\delta + \sqrt{8J^2 + \delta^2})/2|$ of the condition for realization of SRP, which is approximately expanded to $\epsilon \simeq \delta/2 + \sqrt{2}\delta^2/16J$ for a small ratio δ/J . In Fig. 7 we numerically simulate the temporal evolution of populations for states $|00\rangle$, $|01\rangle$, and $|10\rangle$ in the presence of Föster defect $\delta/2\pi = 8.5$ MHz, which shows that our SRP still works because the quantum states are well suppressed to their initial states, although the corresponding values are slightly lower than that in Fig. 2. In this sense we can claim that our scheme is robust against the fluctuation of Föster defect.

Until now we have not considered the spontaneous emissions of the Rydberg states $|p'\rangle$ and $|p''\rangle$, since they are virtually excited in the mechanism of SRP. In this part we take into account both of them in order to give a more convincing result. The lifetimes of Rb $61P_{1/2}$ and $57F_{5/2}$ Rydberg states can be estimated as 0.48 ms and 0.13 ms respectively, from Refs. [45, 47]. By substituting all these factors into the master equation, we plot the corresponding results for controlled- Z gate, ground-state blockade and dissipative entanglement generation in Fig. 8, which are basically consistent with the ideal

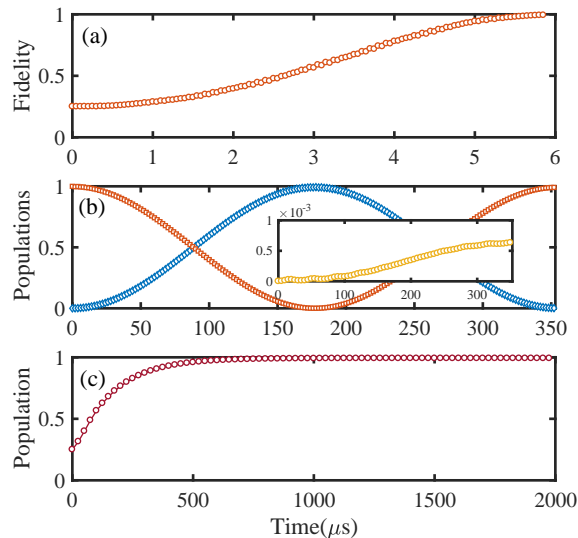


FIG. 8. The temporal evolution of populations for controlled- Z gate, ground-state blockade and dissipative entanglement generation in the presence of Rydberg-state decay, and the parameters are chosen as (a) $\Omega/2\pi = 0.06$ MHz, $\Omega_s/2\pi = 1$ MHz, and $J/2\pi = 50$ MHz; (b) $\Omega_w/2\pi = 0.001$ MHz, $\Omega/2\pi = 0.02$ MHz, $\Omega_s/2\pi = 1$ MHz, and $J/2\pi = 50$ MHz; (c) $\Omega_w/2\pi = 0.005$ MHz, $\Omega/2\pi = 0.01$ MHz, $\Omega_s/2\pi = 1$ MHz, and $J = 100$ MHz.

conditions.

V. SUMMARY

In summary, we have exhibited how to selectly pump the quantum state of neutral atoms using the current technical means and experimental parameters. This SRP mechanism has an analogous form to the Förster resonance interaction, which is very useful for implementation of controlled- Z gate, realization of ground-state blockade, and speedup dissipative entanglement generation. Note that all the parameters in our paper are selected as the simplest time-independent form in order to explain our scheme more clearly. The generalization of our scheme to the cases of soft temporal modulation and multipartite interaction will be investigated in our future study. We hope that our work may provides a new prospect with regard to quantum information processing of neutral atoms.

ACKNOWLEDGMENT

This work is supported by National Natural Science Foundation of China (NSFC) under Grants No. 11774047.

-
- [1] D. Jaksch, J. I. Cirac, P. Zoller, S. L. Rolston, R. Côté, and M. D. Lukin, “Fast quantum gates for neutral atoms,” *Phys. Rev. Lett.* **85**, 2208–2211 (2000).
- [2] M. D. Lukin, M. Fleischhauer, R. Cote, L. M. Duan, D. Jaksch, J. I. Cirac, and P. Zoller, “Dipole blockade and quantum information processing in mesoscopic atomic ensembles,” *Phys. Rev. Lett.* **87**, 037901 (2001).
- [3] E. Urban, T. A. Johnson, T. Henage, L. Isenhower, D. D. Yavuz, T. G. Walker, and M. Saffman, “Observation of rydberg blockade between two atoms,” *Nat. Phys.* **5**, 110–114 (2009).
- [4] Alpha Gaëtan, Yevhen Miroshnychenko, Tatjana Wilk, Amodsen Chotia, Matthieu Viteau, Daniel Comparat, Pierre Pillet, Antoine Browaeys, and Philippe Grangier, “Observation of collective excitation of two individual atoms in the rydberg blockade regime,” *Nat. Phys.* **5**, 115–118 (2009).
- [5] C. Ates, T. Pohl, T. Pattard, and J. M. Rost, “Antiblockade in rydberg excitation of an ultracold lattice gas,” *Phys. Rev. Lett.* **98**, 023002 (2007).
- [6] Thomas Amthor, Christian Giese, Christoph S. Hofmann, and Matthias Weidemüller, “Evidence of antiblockade in an ultracold rydberg gas,” *Phys. Rev. Lett.* **104**, 013001 (2010).
- [7] M. Saffman, T. G. Walker, and K. Mølmer, “Quantum information with rydberg atoms,” *Rev. Mod. Phys.* **82**, 2313–2363 (2010).
- [8] Antoine Browaeys, Daniel Barredo, and Thierry Lahaye, “Experimental investigations of dipole–dipole interactions between a few rydberg atoms,” *Journal of Physics B: Atomic, Molecular and Optical Physics* **49**, 152001 (2016).
- [9] M Saffman, “Quantum computing with atomic qubits and rydberg interactions: progress and challenges,” *Journal of Physics B: Atomic, Molecular and Optical Physics* **49**, 202001 (2016).
- [10] Ditte Møller, Lars Bojer Madsen, and Klaus Mølmer, “Quantum gates and multiparticle entanglement by rydberg excitation blockade and adiabatic passage,” *Phys. Rev. Lett.* **100**, 170504 (2008).
- [11] Xue-Dong Tian, Yi-Mou Liu, Cui-Li Cui, and Jin-Hui Wu, “Population transfer and quantum entanglement implemented in cold atoms involving two rydberg states via an adiabatic passage,” *Phys. Rev. A* **92**, 063411 (2015).
- [12] A. W. Carr and M. Saffman, “Preparation of entangled and antiferromagnetic states by dissipative rydberg pumping,” *Phys. Rev. Lett.* **111**, 033607 (2013).
- [13] Shi-Lei Su, Qi Guo, Hong-Fu Wang, and Shou Zhang, “Simplified scheme for entanglement preparation with rydberg pumping via dissipation,” *Phys. Rev. A* **92**, 022328 (2015).
- [14] X. Q. Shao, J. H. Wu, and X. X. Yi, “Dissipation-based entanglement via quantum zeno dynamics and rydberg antiblockade,” *Phys. Rev. A* **95**, 062339 (2017).
- [15] Yong Zeng, Peng Xu, Xiaodong He, Yangyang Liu, Min Liu, Jin Wang, D. J. Papoular, G. V. Shlyapnikov, and Mingsheng Zhan, “Entangling two individual atoms of different isotopes via rydberg blockade,” *Phys. Rev. Lett.* **119**, 160502 (2017).
- [16] Xiao-Feng Shi, “Universal barenco quantum gates via a tunable noncollinear interaction,” *Phys. Rev. A* **97**, 032310 (2018).
- [17] David Petrosyan and Klaus Mølmer, “Deterministic free-space source of single photons using rydberg atoms,” *Phys. Rev. Lett.* **121**, 123605 (2018).
- [18] A. Omran, H. Levine, A. Keesling, G. Semeghini, T. T. Wang, S. Ebadi, H. Bernien, A. S. Zibrov, H. Pichler, S. Choi, J. Cui, M. Rossignolo, P. Rembold, S. Montangero, T. Calarco, M. En-

- dres, M. Greiner, V. Vuletić, and M. D. Lukin, “Generation and manipulation of schrödinger cat states in rydberg atom arrays,” *Science* **365**, 570–574 (2019).
- [19] T. M. Wintermantel, Y. Wang, G. Lochead, S. Shevate, G. K. Brennen, and S. Whitlock, “Unitary and nonunitary quantum cellular automata with rydberg arrays,” *Phys. Rev. Lett.* **124**, 070503 (2020).
- [20] S.-L. Su, Fu-Qiang Guo, L. Tian, X.-Y. Zhu, L.-L. Yan, E.-J. Liang, and M. Feng, “Nondestructive rydberg parity meter and its applications,” *Phys. Rev. A* **101**, 012347 (2020).
- [21] Suying Bai, Xuedong Tian, Xiaoxuan Han, Yuechun Jiao, Jinhui Wu, Jianming Zhao, and Suotang Jia, “Distinct antiblockade features of strongly interacting rydberg atoms under a two-color weak excitation scheme,” *New Journal of Physics* **22**, 013004 (2020).
- [22] Ulrich Raitzsch, Vera Bendkowsky, Rolf Heidemann, Björn Butscher, Robert Löw, and Tilman Pfau, “Echo experiments in a strongly interacting rydberg gas,” *Phys. Rev. Lett.* **100**, 013002 (2008).
- [23] J. E. Johnson and S. L. Rolston, “Interactions between rydberg-dressed atoms,” *Phys. Rev. A* **82**, 033412 (2010).
- [24] Tyler Keating, Kritika Goyal, Yuan-Yu Jau, Grant W. Biedermann, Andrew J. Landahl, and Ivan H. Deutsch, “Adiabatic quantum computation with rydberg-dressed atoms,” *Phys. Rev. A* **87**, 052314 (2013).
- [25] Weibin Li, Lama Hamadeh, and Igor Lesanovsky, “Probing the interaction between rydberg-dressed atoms through interference,” *Phys. Rev. A* **85**, 053615 (2012).
- [26] S. Möbius, M. Genkin, A. Eisfeld, S. Wüster, and J. M. Rost, “Entangling distant atom clouds through rydberg dressing,” *Phys. Rev. A* **87**, 051602(R) (2013).
- [27] J. B. Balewski, A. T. Krupp, A. Gaj, S. Hofferberth, R. Löw, and T. Pfau, “Rydberg dressing: understanding of collective many-body effects and implications for experiments,” *New Journal of Physics* **16**, 063012 (2014).
- [28] Y.-Y. Jau, A. M. Hankin, T. Keating, I. H. Deutsch, and G. W. Biedermann, “Entangling atomic spins with a rydberg-dressed spin-flip blockade,” *Nat. Phys.* **12**, 71–74 (2016).
- [29] Xiaoqian Chai, Lu Zhang, Dandan Ma, Luyao Yan, Huihan Bao, and Jing Qian, “Anomalous excitation enhancement with rydberg-dressed atoms,” *Phys. Rev. A* **96**, 053417 (2017).
- [30] Jongmin Lee, Michael J. Martin, Yuan-Yu Jau, Tyler Keating, Ivan H. Deutsch, and Grant W. Biedermann, “Demonstration of the jaynes-cummings ladder with rydberg-dressed atoms,” *Phys. Rev. A* **95**, 041801(R) (2017).
- [31] Xiao-Feng Shi and T. A. B. Kennedy, “Simulating magnetic fields in rydberg-dressed neutral atoms,” *Phys. Rev. A* **97**, 033414 (2018).
- [32] Michele Burrello, Igor Lesanovsky, and Andrea Trombettoni, “Reaching the quantum hall regime with rotating rydberg-dressed atoms,” *Phys. Rev. Research* **2**, 023290 (2020).
- [33] Anupam Mitra, Michael J. Martin, Grant W. Biedermann, Alberto M. Marino, Pablo M. Poggi, and Ivan H. Deutsch, “Robust mølmer-sørensen gate for neutral atoms using rapid adiabatic rydberg dressing,” *Phys. Rev. A* **101**, 030301(R) (2020).
- [34] X. Q. Shao, D. X. Li, Y. Q. Ji, J. H. Wu, and X. X. Yi, “Ground-state blockade of rydberg atoms and application in entanglement generation,” *Phys. Rev. A* **96**, 012328 (2017).
- [35] Jeremy Metz and Almut Beige, “Macroscopic quantum jumps and entangled-state preparation,” *Phys. Rev. A* **76**, 022331 (2007).
- [36] R. N. Stevenson, A. R.R. Carvalho, and J. J. Hope, “Production of entanglement in raman three-level systems using feedback,” *Eur. Phys. J. D* **61**, 523–529 (2011).
- [37] D. X. Li and X. Q. Shao, “Unconventional rydberg pumping and applications in quantum information processing,” *Phys. Rev. A* **98**, 062338 (2018).
- [38] Sylvain Ravets, Henning Labuhn, Daniel Barredo, Lucas Béguin, Thierry Lahaye, and Antoine Browaeys, “Coherent dipole-dipole coupling between two single rydberg atoms at an electrically-tuned förster resonance,” *Nat. Phys.* **10**, 914–917 (2014).
- [39] Sylvain Ravets, Henning Labuhn, Daniel Barredo, Thierry Lahaye, and Antoine Browaeys, “Measurement of the angular dependence of the dipole-dipole interaction between two individual rydberg atoms at a förster resonance,” *Phys. Rev. A* **92**, 020701(R) (2015).
- [40] Shi-Lei Su, Erjun Liang, Shou Zhang, Jing-Ji Wen, Li-Li Sun, Zhao Jin, and Ai-Dong Zhu, “One-step implementation of the rydberg-rydberg-interaction gate,” *Phys. Rev. A* **93**, 012306 (2016).
- [41] D. D. Bhaktavatsala Rao and Klaus Mølmer, “Dark entangled steady states of interacting rydberg atoms,” *Phys. Rev. Lett.* **111**, 033606 (2013).
- [42] X. Q. Shao, J. H. Wu, X. X. Yi, and Gui-Lu Long, “Dissipative preparation of steady greenberger-horne-zeilinger states for rydberg atoms with quantum zeno dynamics,” *Phys. Rev. A* **96**, 062315 (2017).
- [43] Dong-Xiao Li, Xiao-Qiang Shao, Jin-Hui Wu, and X. X. Yi, “Dissipation-induced w state in a rydberg-atom-cavity system,” *Opt. Lett.* **43**, 1639–1642 (2018).
- [44] Xiao-Yu Zhu, Zhao Jin, Erjun Liang, Shou Zhang, and Shi-Lei Su, “Preparation of steady 3d dark state entanglement in dissipative rydberg atoms via electromagnetic induced transparency,” *Ann. Phys. (Berlin)* **532**, 2000059 (2020).
- [45] I. I. Beterov, I. I. Ryabtsev, D. B. Tretyakov, and V. M. Entin, “Quasiclassical calculations of blackbody-radiation-induced depopulation rates and effective lifetimes of rydberg ns , np , and nd alkali-metal atoms with $n \leq 80$,” *Phys. Rev. A* **79**, 052504 (2009).
- [46] Xiao-Qiang Shao, “Engineering steady entanglement for trapped ions at finite temperature by dissipation,” *Phys. Rev. A* **98**, 042310 (2018).
- [47] Constantine E. Theodosiou, “Lifetimes of alkali-metal-atom rydberg states,” *Phys. Rev. A* **30**, 2881–2909 (1984).